Electronic Supplementary Material (ESI) for Analyst

Development and applications of a microfluidic reactor with multiple analytical probes

Jesse Greener,*[a] Ethan Tumarkin,*[a] Michael Debono,[a] Chi-Hang Kwan,[b] Milad Abolhasani,[b] Axel Guenther,[b] Eugenia Kumacheva[a,c,]

[a] Department of Chemistry, University of Toronto, 80 Saint George street, Toronto, Ontario, M5S 3H6, Canada

[b] Department of Mechanical and Industrial Engineering, University of Toronto, 5 King's College Road, Toronto, Ontario, M5S 3G8, Canada

[c] Institute of Biomaterials & Biomedical Engineering, University of Toronto, 164 College Street, Toronto, Ontario, M5S 3G9, Canada

1. Schematic of the microfluidic multi-probe channel design

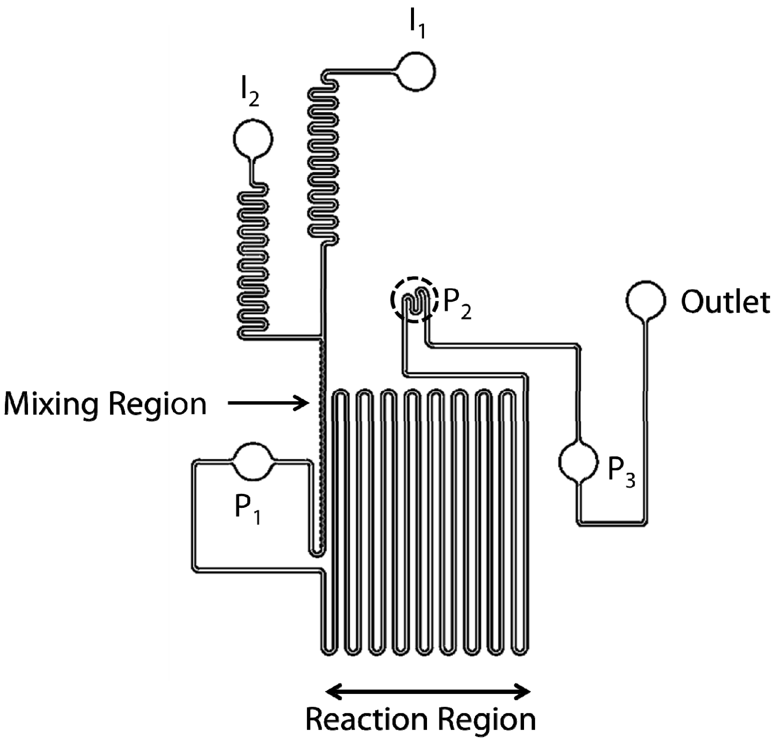

Figure S1. Schematic of the reactor with multiple probes. The positions of probes at points P_1, P_2, and P_3 are 19, 298 and 314 mm, respectively, from the beginning of the mixing region. I_1 and I_2 denote two inlets. The total microchannel length is 331 mm. The height and width of the MF channels were 50 μm and 200 μm, respectively.

2. Probe Design

A customized pH probe was placed in stainless steel tubing with a 1/16″ outer diameter. The home-built thermocouples were placed in 1/16 inch PEEK sheath tubing (part code1538, IDEX Health and Sci.). For both probes the length of the sheath tubing was 2 cm. The tip of the thermocouple probe was immobilized within the sheath tubing using epoxy glue (Speed set epoxy, Lepage), which also provided a leak-proof sealing. The detection elements of the temperature and pH probes were located at the tip of the cylindrical sheath tubing. The pH and temperature probes were inserted into a threaded male plastic connector (modified 10-32 threaded socket head cap screw 3410320037B, McMaster Carr Supply) and polytetrafluoroethylene (PTFE) front ferrule (part code T-103-1, Swagelok).

3. Integration of probes with a MF reactor. Figure SI2 shows a 3D schematic of the components of the MF reactor. The probe connector assembly was interfaced with the threaded (female) ports in the upper polycarbonate layer, which were aligned with probe points in the MF reactor (points P_1, P_2, and P_3 in Fig. SI1) and with inlets I_1, I_2 and Outlet in Fig. SI1. The upper polycarbonate layer was aligned and immobilized above the MF reactor using a clamp (C105-16-401 NW40 clamping ring, Edwards Inc.), which grasped protruding lips that were machined into the upper and lower polycarbonate layers. Tightening the clamp resulted in the compression of the O-rings (Viton 75 Duro, McMaster Carr Supply) against the upper surface of the MF reactor, thereby providing leak-proof sealing. Upon interfacing the probe connector assembly with the MF reactor, the probes extended through the upper polycarbonate layer, so that the detector elements protruded into the microchannel, with the final position shown schematically in Fig 1b. Tightening the connector assembly compressed the ferrule against the sheath tubing. The ATR element interfaced with the MF reactor through the bottom of the microchannel as described elsewhere.[1]

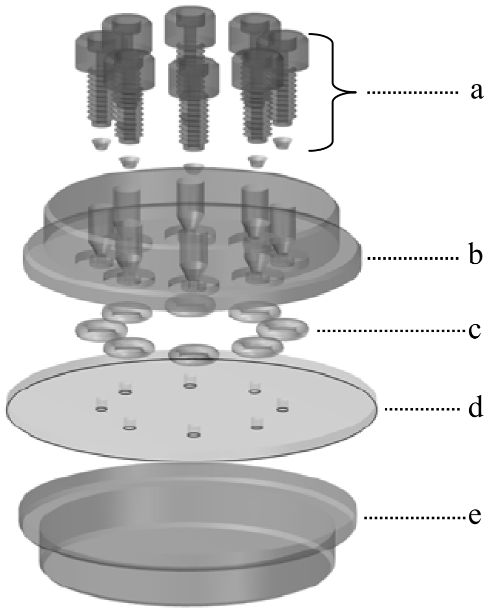

Figure S2. Components of the MF reactor. (a) Threaded connectors and ferrules, (b) upper polycarbonate layer with (female) threaded ports, (c) O-rings, (d) thermoplastic MF reactor, and (e) lower polycarbonate layer.

4. Temperature control and feedback mechanism

Variation in temperature in the MF reactor was achieved by changing the temperature of the heating pad placed either above, or below the MF reactor, that is between layers b and d or between layers d and e, respectively (Fig. SI2). The temperature sensor (k-type thermocouple) was placed into the MF reactor at point P_1 (Fig. 1, main text). Control of temperature of the heating pad was achieved by using the temperature controller (CN79022-C4, Omega Engineering). The integrated thermocouple probe provided constant temperature measurements of the continuous phase, which allowed for temperature modulation of the heating pad. The temperature controller was set to the following settings:

Proportional BW: 0.5°C

Integral Gain: 0.0

Derivative Gain: 0.0

Sensor Type: 15k-1

5. Temperature simulations

We conducted numerical simulations to determine the temperature field inside the MF reactor by using the multiphysics program Comsol (version 4.0a, Comsol, Inc., USA). An unstructured mesh was generated using a resolution of the narrowest region of 0.5. The resultant mesh consisted of 3,756,305 elements. Convective heat loss was considered at all outer surfaces of the MF reactor, that is, on the top and bottom, as well as on the side walls. Boundary conditions were used as follows:

Inlet liquid flow rate: 0.05-10 mL/hr

Outlet pressure: 1 atm (0 kPa gauge pressure)

Liquid inlet temperature: RT = 23 °C

6. Nernstian temperature compensation

The voltage produced at the pH electrode depends on temperature and it is described by the Nernst equation.[2] Therefore, the pH meter was operated in an automatic temperature compensation (ATC) mode, thereby ensuring that temperature-dependent changes to the measured pH arose from the sample, and not the probe. Automatic temperature compensation mode was employed to eliminate apparent changes to the pH value due to temperature dependent changes to the output of the pH electrode.[2]

7. FTIR Spectra:

Fig. SI3(a) shows the FTIR spectrum of a 50 mM Tris buffer solution (pH=7.15) introduced in the MF reactor. The band highlighted at 1060 cm^{-1} (indicated with an arrow) corresponded to the C-N stretching vibrational band. Fig. SI3(b) shows the FTIR spectrum of the same buffer sample after it was saturated with CO_2 to pH=6.4. The peak at 2342 cm^{-1} corresponds to the asymmetric vibration of O-C-O. The intensity of this peak was used, in conjunction with the Beer-Lambert law, for the determination of the concentration of CO_2 (aq).

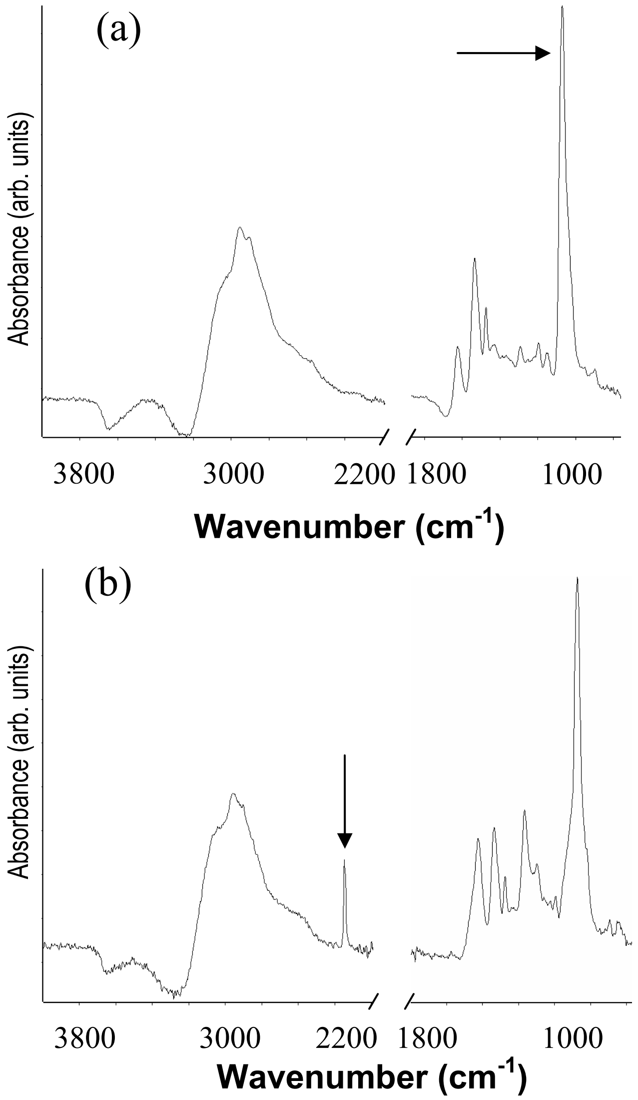

Figure SI 3 (a) FTIR spectrum of 50 mM Tris buffer solution in water (pH=7.15) flowing through the MF reactor at the volumetric flow rate Q=1 mL/hr. (b) FTIR spectrum of CO_2(aq) in Tris buffer (pH=6.4). The spectra shown in (a) and (b) were acquired from a single measurement comprised of 16 scans at 10 kHz and spectral resolution 4 cm^{-1}. The window region of low transmission of the diamond ATR (2200 to 1800 cm^{-1}) has been excluded from both (a) and (b).

References

[1] J. Greener, B. Abbasi and E. Kumacheva, *Lab Chip*, 2010, **10**, 1561-1566.
[2] D. C. Harris, *Quantitative Chemical Analysis*, W. H. Freeman and Co., 2010. pp. 224